

Received: 2018.10.01

Accepted: 2019.01.11

Published: 2019.05.05

# Delayed Contrast Enhancement in Magnetic Resonance Imaging and Vascular Morphology of Primary Diffuse Large B-Cell Lymphoma (DLBCL) of the Central Nervous System (CNS): A Retrospective Study

Authors' Contribution:

Study Design A  
Data Collection B  
Statistical Analysis C  
Data Interpretation D  
Manuscript Preparation E  
Literature Search F  
Funds Collection G

ABCDEF 1,2 **Dandan Liu**  
DEF 2 **Xiaojun Liu**  
DEF 2 **Zhaogui Ba**  
CF 2 **Limei Xie**  
EF 2 **Jiwu Han**  
AF 1 **Dexin Yu**  
A 1 **Xiangxing Ma**

1 Department of Radiology, Qilu Hospital of Shandong University, Jinan, Shandong, P.R. China

2 Department of Radiology, Laigang Hospital Affiliated to Taishan Medical University, Laiwu, Shandong, P.R. China

**Corresponding Authors:** Xiangxing Ma, e-mail: xiangxingma2006@163.com, Dexin Yu, e-mail: yudexin0330@sina.com

**Source of support:** Departmental sources

**Background:** This study aimed to compare the magnetic resonance imaging (MRI) findings of primary diffuse large B-cell lymphoma (DLBCL) of the central nervous system (CNS) with delayed contrast enhancement and histological microvessel density (MVD). T1-weighted and T2-weighted contrast-enhanced and non-enhanced brain imaging were used. CNS lymphoma tissue was evaluated using primary antibodies to endothelial cells and smooth muscle cells, and histochemical staining for reticulin fibers and basement membrane, which allowed quantification of the MVD.


**Material/Methods:** Twenty-one patients with histologically confirmed primary DLBCL of the CNS underwent pre-contrast-enhanced and postcontrast-enhanced MRI. Histology of the CNS lymphoma tissue included immunohistochemical staining with antibodies to CD34 for vascular endothelial cells and alpha smooth muscle actin (ASMA) for vascular smooth muscle cells, and histochemical staining included periodic acid-Schiff (PAS) and silver staining for reticulin fibers to evaluate microvessel density (MVD).

**Results:** In primary DLBCL of the CNS, a positive correlation was found between the degree of necrosis and the size of the lymphoma ( $r=0.546$ ,  $P=0.01$ ). Delayed imaging enhancement was significantly correlated with the number of mature vessels, MVD, basement membrane, and reticulin fibers ( $r=0.593$ ,  $0.466$ ,  $0.446$  and  $0.497$ , respectively). Standardized  $\beta$  regression coefficient analysis showed that the MVD, PAS-positive structures, the number of mature vessels, and reticulin fibers, were significantly associated with delayed enhancement on MRI ( $\beta$  values,  $0.425$ ,  $0.409$ ,  $0.295$ , and  $0.188$ , respectively).

**Conclusions:** In primary DLBCL of the CNS, delayed imaging enhancement on MRI may be due to reduced neovascularization and vascular infiltration by lymphoma cells.

**MeSH Keywords:** Brain Neoplasms • Endothelium, Vascular • Lymphoma, B-Cell • Magnetic Resonance Imaging • Reticulin

**Full-text PDF:** <https://www.medscimonit.com/abstract/index/idArt/913439>

 3343

 2

 1

 27



## Background

Primary non-Hodgkin's lymphoma (NHL) of the central nervous system (CNS) is uncommon, accounting for 1–3% of all intracranial malignant neoplasms and 1–2% of all lymphomas [1–5]. However, an increasing incidence has been reported of primary NHL of the CNS in both immunocompetent and immunodeficient patients [6–10]. Most primary CNS lymphomas are usually high-grade, B-cell NHL, which includes primary diffuse large B-cell lymphoma (DLBCL) of the CNS. Due to the chemosensitivity and radiosensitivity of primary high-grade B-cell lymphomas of the CNS, surgical management is usually avoided [4,11]. Therefore, the accurate diagnosis of primary B-cell lymphoma, including primary DLBCL of the CNS, is crucial for the patient management, and imaging techniques play an important diagnostic role.

Primary DLBCL of the CNS is associated with invasion into the perivascular space and infiltration into the blood vessel wall, resulting in damage of the blood-brain barrier [12]. Edema and small molecules, including contrast agents, can easily permeate into the extravascular space of the lymphoma and the neighboring tissue and enter the interstitial space. Therefore, primary DLBCL of the CNS should present with marked contrast-enhancement on imaging at the early stage. However, in clinical practice, primary DLBCL of the CNS is associated with hypoperfusion on contrast-enhanced computed tomography (CT) or magnetic resonance imaging (MRI) in the early stages, indicating reduced oxygenation of the arterial blood supply, but with less necrosis, which is a contradictory finding. Also, most cases of primary DLBCL of the CNS show marked enhancement in the delayed phase on MRI, but the underlying mechanism remains unclear. One possible mechanism, which was evaluated in this study, is vasculogenic mimicry, which is a term that describes the development of vascular-like structures or vascular channels without the presence of endothelial cells in highly aggressive malignant tumors.

Therefore, this study aimed to compare the magnetic resonance imaging (MRI) findings of primary diffuse large B-cell lymphoma (DLBCL) of the central nervous system (CNS) with delayed contrast enhancement and histological microvessel density (MVD). T1-weighted and T2-weighted contrast-enhanced and non-enhanced brain imaging were used. CNS lymphoma tissue was evaluated using primary antibodies to endothelial cells and smooth muscle cells, and histochemical staining for reticulin fibers and basement membrane, which allowed quantification of the MVD.

## Material and Methods

### Patients

This retrospective study included 21 patients with primary diffuse large B-cell lymphoma (DLBCL) of the central nervous

system (CNS), confirmed by histopathology, who were enrolled from August 1<sup>st</sup>, 2012 to October 30<sup>th</sup>, 2016. The study population included 13 men and 8 women with an age range of 31–76 years (mean age, 55.95 years). The local Ethics Committee of Qilu Hospital of Shandong University, Jinan, China approved the study (Approval No. 2017091).

In addition to a histologically confirmed diagnosis of DLBCL of the CNS, the study included patients who underwent bone marrow cytology and other examinations to exclude systemic or non-primary CNS lymphoma. The study exclusion criteria were patients with a history of acquired immunodeficiency syndrome (AIDS), or congenital immunodeficiency disorders, or incomplete information of magnetic resonance imaging (MRI), who were without clinical data, or who had hormone and anti-lymphoma therapy before MRI examination. All patients underwent pre-contrast and post-contrast enhanced MRI examination and received the results within two weeks following MRI. In the 21 patients included in the study, 16 patients underwent surgery and five patients underwent CT-guided stereotactic needle biopsy, and all had histologically confirmed primary DLBCL of the CNS. The clinical manifestations of the patients were recorded and included dizziness, headache, limb dysfunction, visual field defect, and fever.

### Magnetic resonance imaging (MRI)

MRI was performed using a Signa 1.5 T system (GE Healthcare Life Sciences, Logan, UT, USA). Pre-contrast axial T1-weighted imaging was performed with a repetition/echo time (TR/TE) of 450/10 ms, a field of view (FOV) of 240×240 mm, imaging section thickness of 5 mm, intersection gap of 1.0 mm, number of excitations (NEX) 1.5, and a matrix 256×192. Pre-contrast axial T2-weighted imaging was performed with a TR/TE of 4200/98 ms, a FOV of 240×240 mm, a section thickness 5 mm, an intersection gap of 1.0 mm, NEX 1.5, and a matrix 256×192.

Contrast enhancement was performed using Magnevist® (gadopentetate dimeglumine) (0.1 mmol/kg) (Bayer Healthcare, Leverkusen, Germany), which was injected into the median cubital vein by nursing staff. All patients had no contraindications for the examination and were required to fast for at least four hours before imaging. Conventional contrast-enhanced coronal, sagittal, and axial MRI imaging was performed.

### Image analysis

Observation and measurement of all images from patients with primary DLBCL of the CNS were performed by consensus between two radiologists with nine and eleven years of experience, respectively, who were unaware of the clinical details of the patients, and the purpose of the study. The magnetic resonance (MR) images were stored in the picture archiving and communication system (PACS) and were transmitted to

an MRAW4.3 workstation (GE Healthcare Life Sciences, Logan, UT, USA) for analysis. For the delayed enhanced images, the last axial T1-weighted image was used to evaluate the imaging features with a delayed time of more than 3 min. For multiple lesions, only the largest lesion underwent needle biopsy. MRI units were analyzed for primary DLBCL of the CNS and normal white matter in three regions of interest (ROI) on pre-contrast axial T1-weighted imaging and delayed-enhanced T1-weighted images, and the average values were calculated.

For each brain lesion, the MRI enhanced index (EI) was calculated according to the formula:  $EI = V_1/V_2 - V_3/V_4$ , where the  $V_1$  and  $V_2$  were the MR units of primary DLBCL of the CNS and white matter after enhancement, respectively.  $V_3$  and  $V_4$  were the MR units of primary DLBCL of the CNS and white matter before and after enhancement, respectively.

Other MRI features of the brain lesions were evaluated, including position, shape, size, necrosis within the lymphoma, infiltration to the neighboring meninges, enhancing homogeneity, notch sign, and sharp angle sign. Infiltration of the meninges appeared as linear or nodular enhancement of the meninges around the lesion. The grade of necrosis (N) was calculated according to the formula for the EI, and  $V_1$  was the volume of tumor and  $V_2$  was the volume of necrosis in the lymphoma. Necrosis (N)  $< 1/3$  represented mild necrosis, N  $< 2/3$  represented moderate necrosis, and N  $\geq 2/3$  represented severe necrosis.

### Histology, histochemistry, and immunohistochemistry

Tissue sections of the brain biopsy samples were prepared using routine fixation, and tissue sections were cut from formalin-fixed, paraffin wax-embedded tissue blocks and stained routinely for light microscopy using hematoxylin and eosin (H&E) staining. To evaluate the microvasculature within the lymphoma, reticulin fibers (type III collagen secreted by reticular cells) were stained histochemically using Gordon and Sweet's silver staining method, and periodic acid-Schiff (PAS) was used to evaluate vascular basement membrane.

Routine immunohistochemistry was used, with positive and negative controls, and primary antibodies to CD34 for endothelial cells, and alpha smooth muscle actin (ASMA) for vascular smooth muscle cells. Double immunohistochemical and histochemical staining was performed with CD34 and PAS.

After reviewing the immunostained sections at low magnification, three areas of the lymphoma tissue with the greatest number of distinctly highlighted areas (hotspots), or the interface areas between the lymphoma and normal brain tissue (interface), the microvessel density (MVD) was measured at an objective magnification of  $\times 200$ . The method of quantifying MVD ( $\text{mm}^2$ ) was as previously described [14]. Light microscopy

observation was performed in five randomly chosen fields. If PAS-positive vascular structures were identified in three or more fields and accounted for more than half of each field, the MVD was considered to be strongly positive (grade II); otherwise, it was weakly positive (grade I). The distribution of the reticulin fibers in the lymphoma was observed in five random high-power fields ( $\times 400$ ). If the reticulin appeared in three or more fields and accounted for more than half of each field, it was considered as strongly positive (grade II). Otherwise, it was weakly positive (grade I).

### Statistical analysis

Data were analyzed using SPSS version 19.0 software. For histological and MRI findings, correlation analysis and multiple linear regression analysis were used. Multiple linear regression analysis was used to analyze the relationship between the

enhancement of the primary DLBCL of the CNS and the PAS-positive histochemical staining pattern, the MVD, and the number of mature vessels. The Shapiro-Wilk test of normality was used.  $P < 0.05$  was considered statistically significant.

## Results

### Magnetic resonance imaging (MRI)

On magnetic resonance imaging (MRI), 21 patients had 37 lesions of primary diffuse large B-cell lymphoma (DLBCL) of the central nervous system (CNS) were found including 14 solitary lesions, and there were 23 multiple foci of lymphoma in seven patients. For the solitary lesions of lymphoma, six were located in the frontal lobe, and involved the corpus callosum in one patient, the temporal lobe in three patients, the in occipital lobe in two patients, the cerebellar hemisphere in one patient, the tentorium cerebelli in one patient, and the basal ganglia in one patient. The multiple lesions were mainly located in the frontal, parietal, basal ganglia, and corpus callosum regions.

The maximum diameter of the foci of brain lymphoma imaged in the 21 patients included in the study ranged from 1.0–7.5 cm with a mean diameter of  $3.68 \pm 1.51$  cm. There was one lesion with ring-like enhancement, the other lesions were nodular, with mass-like enhancement on delayed enhanced imaging (Figure 1A–1C). The MRI enhanced index (EI) was 0.45–1.65, with a mean value of  $0.998 \pm 0.370$ , and in nine lesions, the EI was  $< 1.0$ .

There were 13 lesions of cerebral lymphoma with a notch sign, seven lesions with sharp angle sign, and six lesions with a fist sign. Meningeal infiltration was identified in four lesions. There

were nine lesions with necrosis, seven of which showed mild necrosis, with small cysts in three lesions, one showed moderate necrosis, and the remaining lesion showed severe necrosis. There was a significant positive correlation between intra-lymphoma necrosis and the size of the lesion ( $r=0.546$ ,  $P=0.01$ ). No necrosis was found in lesions of intracerebral lymphoma with a maximum diameter  $<2.5$  cm.

### Histology and immunohistochemistry

Routine histology of the tissue sections, stained with hematoxylin and eosin (H&E), showed that the lymphoma cells were large, round or oval, with an increased nuclear to cytoplasm ratio, closely arranged, with round or oval nuclei (Figure 1D). Combined immunohistochemistry and histochemistry for CD34 and PAS staining showed that the microvessel density (MVD) ranged from  $16.67-85.33/\text{mm}^2$  (Figure 1E), with a mean MVD of  $43.40 \pm 19.68/\text{mm}^2$ .

Alpha smooth muscle actin (ASMA) immunostaining showed that the number of mature vessels, containing smooth muscle cells, ranged from between  $3-17.67/\text{mm}^2$ , and the mean number of mature vessels was  $9.68 \pm 4.08/\text{mm}^2$ . Lymphoma cells were arranged in concentric circles around blood vessels (Figure 1F). Also, the reticulin fibers (type III collagen secreted by reticular cells) was found in the lesions of cerebral lymphoma, and a concentric perivascular reticular fiber network was seen (Figure 1G). Eleven lesions were strongly positive, and 10 lesions were weakly positive for reticulin staining. Combined immunohistochemistry and histochemistry staining with CD34 and PAS showed that 21 lesions were PAS-positive, 12 of which were strongly positive, and the PAS-positive structures were connected together to form a network (Figure 1H); nine lesions were weakly positive and linear, with branching PAS-positive patterns. In the PAS-positive structures, there were adjacent vascular loops and some small channels were surrounded by lymphoma cells, with or without a layer of PAS-positive basal membrane (Figure 1I).

Analysis with the independent sample t-test showed that the MRI enhanced index (EI) of primary DLBCL of the CNS was significantly different compared with the PAS staining ( $t=-2.768$ ,  $P=0.012$ ); the EI of primary DLBCL of the CNS was significantly different compared with the reticulin staining ( $t=-2.323$ ,  $P=0.031$ ) (Table 1).

Statistical analysis using the Shapiro-Wilk test showed that the EI and the number of mature vessels of primary DLBCL of the CNS conformed to a normal distribution and the MVD did not conform to a normal distribution ( $P=0.026$ ). Therefore, Pearson's correlation analysis showed that the EI was significantly correlated with the number of mature vessels (containing smooth muscle cells) ( $r=0.593$ ,  $P=0.005$ ). Spearman's

correlation analysis showed that the MVD, the number of PAS-positive structures, and reticulin fibers were significantly correlated with the EI ( $\rho=0.466$ ,  $0.581$ , and  $0.497$ ;  $P<0.05$ ). Multiple linear regression analysis showed a significant positive correlation between the EI and the PAS-positive structures, the MVD, the number of mature vessels, and the number of reticulin fibers ( $R^2=0.75$ ;  $F=12.09$ ;  $P<0.001$ ). The regression equation was:  $Y=-0.285-0.08X_1+0.136X_2+0.299X_3+0.027X_4$  (where  $X_1$  was MVD,  $X_2$  was reticulin fibers,  $X_3$  was PAS staining,  $X_4$  was the number of mature vessels).

### Correlation of the delayed MRI features with MVD, the PAS-positive vascular pattern and the number of mature vessels

The factors that influenced the delayed enhancement of primary DLBCL of the CNS on MRI imaging were MVD, the presence of PAS-positive structures, the number of mature vessels, and reticulin fibers, which has standardized regression coefficients ( $\beta$ ) of  $0.425$ ,  $0.409$ ,  $0.295$ , and  $0.188$ , respectively (Table 2).

## Discussion

Primary diffuse large B-cell lymphoma (DLBCL) of the central nervous system (CNS) is an uncommon subtype of extranodal non-Hodgkin's lymphoma (NHL) that involves the CNS, without evidence of systemic disease [5,10]. Most cases of primary CNS lymphoma are B-cell lymphomas, and T cell lymphomas are very rare [1,7]. In this study, all 21 patients had a histologically-confirmed diagnosis of diffuse large B-cell lymphoma (DLBCL), which was mainly supratentorial and distributed in the deep white matter. Magnetic resonance imaging (MRI) showed the typical features of primary DLBCL of the CNS with a homogeneous signal on T1-weighted imaging and a hypointense or isointense signal. On T2-weighted imaging, or the T2 fluid-attenuated inversion recovery (FLAIR) sequence, primary DLBCL of the CNS appeared to be isointense or had a slightly hyperintense signal, and diffusion-weighted MRI was hyperintense.

Previously published studies on the contrast-enhanced MRI characteristics of primary DLBCL of the CNS, have shown that the contrast agents diffuse into the extracellular space through the damaged blood-brain barrier, resulting in enhancement on imaging [12,15-18]. However, these previous studies have also shown that the time-intensity curve (TIC) of primary DLBCL of the CNS slowly increased [18,19], which indicated that there was low enhancement and low perfusion of primary DLBCL of the CNS at the early enhanced phase [18-20].

The findings of the present study showed that in primary DLBCL of the CNS with poor vasculature identified by histology, the microvessel density (MVD) was only  $43.40/\text{mm}^2$ , and the number



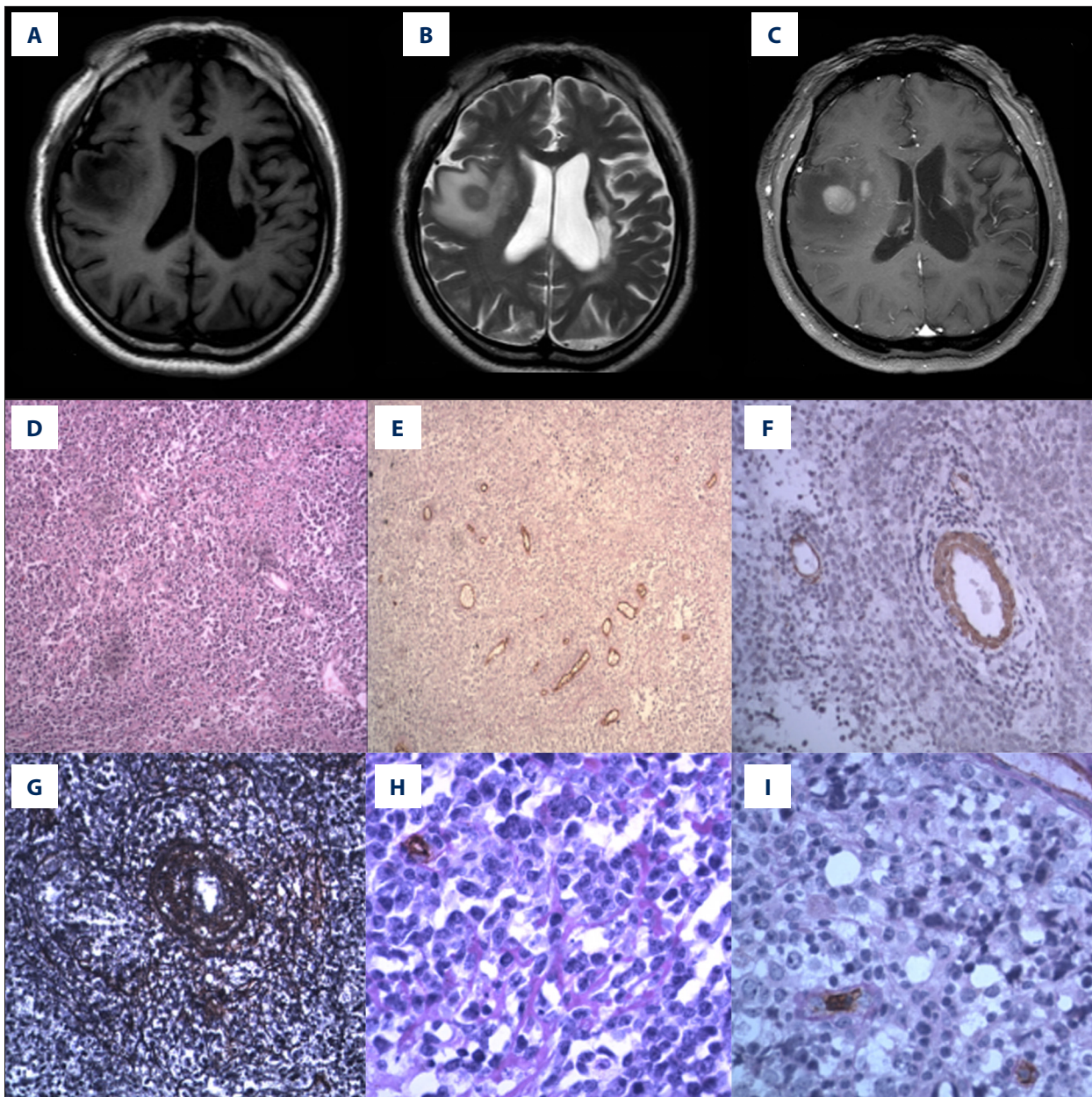


**Figure 1.** A 56-year-old man with lymphoma involving right temporal lobe. Coronal brain magnetic resonance imaging (MRI) and photomicrographs of the histology and immunohistochemistry. **(A)** Pre-contrast T1-weighted magnetic resonance image (MRI) of the brain. **(B)** Pre-contrast T2-weighted magnetic resonance image (MRI) of the brain. **(C)** Post-contrast T1-weighted magnetic resonance image (MRI) of the brain. **(D)** Photomicrograph of the histology of the cerebral lymphoma tissue shows large cells that are round or oval, with enlarged round or oval cell. Hematoxylin and eosin (H&E). Magnification  $\times 100$ . **(E)** Photomicrograph of the immunohistochemical staining of the vascular endothelial cells (blue arrow) for CD34 expression in the cerebral lymphoma tissue shows microvessel density (MVD)=33.66/mm<sup>2</sup>. Periodic acid-Schiff (PAS). Magnification  $\times 100$ . **(F)** Photomicrograph of the immunohistochemical staining of smooth muscle cells for alpha smooth muscle actin (ASMA) expression in the cerebral lymphoma tissue shows that the number of mature vessels in the lymphoma was 8/mm<sup>2</sup>. Magnification  $\times 200$ . **(G)** Photomicrograph of the silver staining for reticulin fibers in the cerebral lymphoma tissue shows the concentric perivascular reticular fiber network (white arrow). Magnification  $\times 200$ . **(H)** Photomicrograph of the immunohistochemical staining of the vascular endothelial cells for CD34 expression in the cerebral lymphoma tissue combined with periodic acid-Schiff (PAS) (red staining) shows the basal membrane (black arrow). Magnification  $\times 400$ . **(I)** Photomicrograph of the immunohistochemical staining of the vascular endothelial cells for CD34 expression in the cerebral lymphoma tissue combined with periodic acid-Schiff (PAS) (red staining) shows the basal membrane (yellow arrow). Magnification  $\times 400$ .

**Table 1.** The magnetic resonance imaging (MRI) enhanced index (EI) of primary diffuse large B-cell lymphoma (DLBCL) of the central nervous system (CNS) and the histology of the periodic acid-Schiff (PAS)-positive structures and reticulin fibers.

		$\bar{x}\pm SD$	t	P
PAS-positive structure	Grade I	0.77±0.39	-2.768	0.012
	Grade II	1.17±0.25		
Reticulin fibers	Grade I	0.82±0.36	-2.323	0.031
	Grade II	1.16±0.31		

**Table 2.** Correlation of the magnetic resonance imaging (MRI) features with the microvessel density (MVD), periodic acid-Schiff (PAS)-positive structures and the number of mature vessels.

	Correlation coefficient	P#	B	β	P*
PAS-positive structures	0.581	0.043	0.129	0.409	0.036
MVD	0.466	0.002	0.008	0.425	0.031
Mature vessels	0.593	0.005	0.016	0.295	0.120
Reticulin	0.497	0.022	0.299	0.188	0.309

P# – P-value of the correlation analysis; P\* – P-value of multiple linear regression analysis; B – the regression coefficient; β – the standardized regression coefficient; MVD – microvessel density; PAS – periodic acid-Schiff.

of mature vessels was 9.68/mm<sup>2</sup>. Liao [18] reported that primary DLBCL of the CNS had a significantly lower MVD when compared with high-grade glioma. These findings might explain why primary DLBCL of the CNS has low perfusion. However, the lack of vessels result in reduced delivery of contrast agent into the lymphoma, resulting in delayed imaging enhancement, but does not explain why primary DLBCL of the CNS has so little necrosis. Therefore, it might be possible that other factors are involved in the findings on contrast-enhanced MRI. The findings of the present study showed that there were different types and number of PAS-positive structures in primary DLBCL of the CNS, and these PAS-positive structures, that were non-endothelial cell lined, were thickened, and formed adjacent small circular structure surrounded by lymphoma cells, and delayed imaging enhancement was associated with these PAS-positive structures.

Vasculogenic mimicry is a term that describes the development of vascular-like structures without the presence of endothelial cells in highly aggressive malignant tumors, and it is possible that this phenomenon occurs in high-grade lymphoma [21,22]. Therefore, in contrast-enhance MRI, the contrast agent could enter into the new vascular channels, or vascular-like structures, accompanied by plasma. Because the vascular channels seen in vasculogenic mimicry have no endothelial cells or tight junctions, the blood-brain barrier is breached and the contrast agent can permeate into the extracellular space between the lymphoma cells. Theoretically, the destruction of

the blood-brain barrier can promote the rapid dispersion of contrast agents, but the primary DLBCL of the CNS does not show early enhancement but a marked delayed enhancement.

The question remains as to what causes the delayed enhancement of primary DLBCL of the CNS. The findings of the present study showed that in primary DLBCL of the CNS, lymphoma cells were closely arranged closely and the extracellular space was small, which might result in impaired diffusion of the contrast agent. Also, this study showed the presence of a rich reticulin fiber network in primary DLBCL of the CNS, consisting of a concentric perivascular reticulin fiber network, which has previously been reported to be a typical feature of primary DLBCL of the CNS [23]. Reticulin is type III collagen secreted by reticular cells. Therefore, these factors may have resulted in a gradual accumulation of interstitial contrast agent, leading to slow wash-in and slow wash-out, and typical delayed enhancement of the imaging lesions of primary DLBCL of the CNS.

The growth and metastasis of malignant tumors, including lymphoma, depend on the tumor blood supply. If there is not enough blood supply to meet the rapid growth of the lymphoma, it will undergo necrosis. Primary DLBCL of the CNS was found to be hypovascular and had a reduced MVD. However, the findings of this study also showed that most of the primary CNS lesions of DLBCL showed mild necrosis on MRI, only one case had severe necrosis, and necrosis was found when the size of the lymphoma was >2.5 cm.

However, the co-existence of hypovascularity with reduced necrosis appears contradictory. Previously published studies have explained this finding in terms of damage to the blood-brain barrier occurring in the lymphoma, resulting in leakage of nutrients and oxygen that reduce the degree of necrosis and result in marked enhancement on MRI [11,15,18]. However, the limited number of blood vessels are likely to limit the leakage of nutrients and oxygen, which is supported by hypoperfusion on CT or MRI. Also, the rich reticulin fiber network and hypercellularity within the lymphoma are more likely to impede the diffusion of oxygen and nutrients. Therefore, damaged blood-brain barrier and leakage do not seem to adequately explain the apparent contradictions between hypovascularity and hypoperfusion, reduced necrosis, and delayed contrast-enhancement.

However, in addition to angiogenic blood vessels, and mature blood vessels, the process of vasculogenic mimicry, or the development of vascular-like structures or vascular channels without the presence of endothelial cells, can deliver red blood cells, plasma, oxygen, and nutrients to the lymphoma tissue. Vasculogenic mimicry might explain the reduced necrosis and delayed imaging enhancement of DLBCL of the CNS. The present study showed that out of 21 lesions, necrosis was found in nine lesions, which was higher than previously reported [24–27]. In the present study, the lymphoma lesions with necrosis had a larger diameter. This imaging finding might be supportive for the diagnosis of primary DLBCL of the CNS. This study showed that necrosis was not related to lymphoma MVD and the number of mature vessels, which supports a role for vasculogenic mimicry.

## References:

1. Haldorsen IS, Krossnes BK, Aarseth JH et al: Increasing incidence and continued dismal outcome of primary central nervous system lymphoma in Norway 1989–2003: Time trends in a 15-year national survey. *Cancer*, 2007; 110(8): 1803–14
2. Coulon A, Lafitte F, Hoang-Xuan K et al: Radiographic findings in 37 cases of primary CNS lymphoma in immunocompetent patients. *Eur Radiol*, 2002; 12: 329–40
3. Villano JL, Koshiy M, Shaikh H et al: Age, Gender, and racial differences in incidence and survival in primary CNS lymphoma. *Br J Cancer*, 2011; 105(9): 1414–18
4. Citterio G, Renia M, Gattab G et al: Primary central nervous system lymphoma. *Hematology*, 2017; 113: 97–110
5. Burton EC, Ugiliweneza B, Kolikonda MK et al: A regional multicenter retrospective analysis of patients with primary central nervous system lymphoma diagnosed from 2000–2012: Treatment patterns and clinical outcomes. *Cureus*, 2017; 9(7): e1512
6. Zhang D, Hu LB, Henning TD et al: MRI findings of primary CNS lymphoma in 26 immunocompetent patients. *Korean J Radiol*, 2010; 11(3): 269–77
7. Olson JE, Janney CA, Rao RD et al: The continuing increase in the incidence of primary central nervous system non-Hodgkin lymphoma: A surveillance, epidemiology, and end results analysis. *Cancer*, 2002; 95(7): 1504–10
8. Takeuchi H, Matsuda K, Kitai R et al: Angiogenesis in primary central nervous system lymphoma. *J Neurooncol*, 2007; 84: 141–45
9. Eloranta S, Branvall E, Celsing F et al: Increasing incidence of primary central nervous system lymphoma but no improvement in survival in Sweden 2000–2013. *Eur J Haematol*, 2018; 100(1): 61–68
10. Enblad G, Martinsson G, Baecklund E et al: Population-based experience on primary central nervous system lymphoma 2000–2012: The incidence is increasing. *Acta Oncol*, 2017; 56(4): 599–607
11. Dubuisson A, Kaschten B, Le'nelle J et al: Primary central nervous system lymphoma report of 32 cases and review of the literature. *Clin Neurol Neurosurg*, 2004; 107: 55–63
12. Cheng G, Dong C, Zhang LM et al: Imaging features of primary central nervous system lymphoma. *Chin J Neurosurg Dis Res*, 2015; 14(6): 490–93
13. The Chinese Neurosurgery Society: Expert consensus on the treatment of edema around intracranial tumors (1). *Natl Med J China*, 2010; 90(1): 5–9
14. Sugita Y, Takase Mori D et al: Endoglin (CD 105) is expressed on endothelial cells in the primary central nervous system lymphomas and correlates with survival. *J Neurooncol*, 2007; 82: 249–56
15. Partovi S, Karimi S, Lyo JK et al: Multimodality imaging of primary CNS lymphoma in immunocompetent patients. *Br J Radiol*, 2014; 87(1036): 20130684
16. Kuler WN, Gele T, Korfel A et al: Primary central nervous system lymphomas (PCNSL): MRI features at presentation in 100 patients. *J Neurooncol*, 2005; 72(2): 169–77
17. Eichler AF, Batchelor TT: Primary central nervous system lymphoma: Presentation, diagnosis and staging. *Neurosurg Focus*, 2006; 21(5): E15
18. Liao WH, Liu YH, Wang XY et al: Differentiation of primary central nervous system lymphoma and high-grade glioma with dynamic susceptibility contrast-enhanced perfusion magnetic resonance imaging. *Acta Radiol*, 2009; 50(2): 217–25

## Conclusions

A retrospective study combined computed tomography (CT) and magnetic resonance imaging (MRI) with vascular morphology in cases of primary diffuse large B-cell lymphoma (DLBCL) of the central nervous system (CNS). The findings showed that hypovascularity of DLBCL but the presence of vascular structures without an endothelial cell lining, or vasculogenic mimicry, were associated with delayed contrast enhancement but less necrosis. These results may help to explain the imaging findings in primary DLBCL of the CNS and highlight some important diagnostic features of primary DLBCL of the CNS seen on imaging.

## Conflict of interest

None.



19. Sugahara T, Korogi Y, Shigematsu Y et al: Perfusion-sensitive MRI of cerebral lymphomas: A preliminary report. *J Comput Assist Tomogr*, 1999; 23: 232–37
20. Zacharia TT, Law M, Naidich TP et al: Central nervous system lymphoma characterization by diffusion-weighted imaging and MR spectroscopy. *J Neuroimaging*, 2008; 18(7): 411–17
21. Maniotis AJ, Folberg R, Hess A et al: Vascular channel formation by human melanoma cells *in vivo* and *in vitro* vasculogenic mimicry. *Am J Pathol*, 1999; 155(3): 739–52
22. Cai XS, Jia YW, Mei J et al: Tumor blood vessels formation in osteosarcoma: Vasculogenesis mimicry. *Chin Med J (Engl)*, 2004; 117(1): 94–98
23. Blasel S, Jurcoane A, Bähr O et al: MR perfusion in and around the contrast-enhancement of primary CNS lymphomas. *J Neurooncol*, 2013; 114: 127–34
24. Tang YZ, Booth TC, Bhogal P et al: Imaging of primary central system lymphoma. *Clin Radiol*, 2011; 66(8): 768–77
25. Jenkins CN, Colquhoun IR: Characterization of primary intracranial lymphoma by computed tomography: An analysis of 36 cases and a review of the literature with particular reference to calcification haemorrhage and cyst formation. *Clin Radiol*, 1998; 53: 428–34
26. Lu S, Wang S, Gao Q et al: Quantitative evaluation of diffusion and dynamic contrast-enhanced magnetic resonance image for differentiation between primary central nervous system lymphoma and glioblastoma. *J Comput Assist Tomogr*, 2017; 41(6): 898–903
27. Taskinen M, Jantunen E, Kosma VM et al: Prognostic impact of CD31-positive microvessel density in follicular lymphoma patients treated with immunochemotherapy. *Eur J Cancer*, 2010; 46: 2506–12